Journal of Optoelectronics and Advanced Materials Vol. 7, No. 6, December 2005, p. 3039 - 3046

OPTICAL AND TRANSPORT PROPERTIES OF UNDOPED AND Al-, Ga- AND In-DOPED ZnO THIN FILMS

L.-S. Hsu*, C. S. Yeh[a], C. C. Kuo[b], B. R. Huang[c], S. Dhar[d]

Division of Physical Sciences, University of Guam, Guam 96923, USA
[a]Graduate School of Engineering Science and Technology, National Yunlin University of Science and Technology, Touliu, Taiwan, R.O.C.
[b]Department of Industrial Education and Technology, National Changhua University of Education, Changhua, Taiwan, R.O.C.
[c]Department of Electronic Engineering, National Yunlin University of Science and Technology, Touliu, Taiwan, R.O.C.
[d]Department of Electronic Science, University of Calcutta, Calcutta-700 009, India

Pulsed-laser deposition of undoped and Al-, Ga- and In-doped ZnO thin films is reported. The structure of the films remained unaffected by doping. The effect of doping on the optical and transport properties of the films was investigated. The band gaps, the optical constants, and the electron concentrations of the ZnO films are obtained from the ellipsometry and spectrophotometry data. Blue shift of the band gap due to doping is observed. The Burstein-Moss effect is remarked in the Ga- and In-doped ZnO films. The transport data show the increase of conductivity and mobility by doping with Al, Ga, or In. A number of deep levels with energies ranging from 0.75 to 1.14 eV are found in the ZnO films by photoconductivity measurement.

(Received November 9, 2005; accepted November 24, 2005)

Keywords: ZnO films, Doping by Al, Ga, In, Pulsed laser deposition

1. Introduction

ZnO is one of the II-VI materials used for the fabrication of functional devices such as surface acoustic-wave devices, gas sensors, and transparent conducting layers [1]. The observation of UV light emission from ZnO thin films by laser excitation has triggered an intense research activity in this and related materials [2-5]. The various properties of ZnO are very similar to those of GaN, which makes ZnO a technologically important material for making light emitting diodes and lasers [2]. Compared with magnetron sputtering and reactive RF-sputtering techniques, pulsed laser deposition (PLD) is an attractive technique for the deposition of ZnO thin films with excellent structural homogeneity and crystalline quality. However, technological problems and challenges still exist for using this technique to grow ZnO films with optical and electrical properties suitable for device applications. Specific deposition conditions and annealing procedures are to be developed for controlling the formation of clusters and aggregates to suppress the spurious nucleation in the ZnO films [3,4]. Research efforts are underway using a variety of substrates and different growth conditions to improve these properties [5,6]. The effect of oxygen partial pressure, doping, and annealing condition on the growth of ZnO thin films was extensively studied [7]. As was used as dopant in ZnO thin films to tailor the material properties [8] Studies on sputtered- and PLD-grown Al-doped ZnO films were reported earlier [9,10]. Yamamoto et. al. [11,12] calculated the change of Madelung energy of ZnO by doping. Shim et. al. [13] reported the effect of post-deposition annealing temperatures on the light-emitting property of ZnO film. The increase of electrical

* Corresponding author: phhsu@yahoo.com

conductivity without impairing optical transmission by doping was discussed by Zeuner et. al. [14] P-type ZnO films were grown using co-doping technique, and the optical properties of undoped and Al-doped ZnO thin films were reported [15,16]. Study on ZnO films deposited on various substrates (Si, Al_2O_3, and Corning glass) was also reported [17]. E. de Posada et. al. [18] deposited thin films of ZnO and $Zn_{1-x}Mn_xO$ (x=0.13) on sapphire substrate and studied the effects of target-to-substrate distance and oxygen partial pressure. These studies indicate that a comprehensive understanding is yet to be achieved on the effect of doping ZnO with group III metals to its physical properties.

In this study, we report the deposition of a series of undoped and Al-, Ga- and In-doped ZnO thin films on glass substrate by PLD and their characterizations using X-ray diffraction (XRD), atomic force microscopy (AFM), and optical and transport measurements. Experiments on the growth of undoped and doped ZnO films under varying deposition temperatures, oxygen partial pressures, and dopant materials were carried out to achieve the optimal deposition condition. Crystallinity quality and surface morphology of the ZnO films were correlated with their optical and transport properties. The occurrence of various optically active deep levels in undoped and doped ZnO thin films is also explored.

2. Experiments

Pulsed excimer laser (KrF, λ=248 nm) with repetition rate of 10-20 Hz was used for the deposition of ZnO films. Sintered ZnO target of 5N purity was placed on a rotating holder. The glass substrate was cleaned with acetone for 20 minutes in an ultrasonic cleaner and dried prior to mounting on the sample holder. A target-to-substrate distance was kept at 3 cm. Base pressure of 10^{-5} to 10^{-6} Torr in the vacuum chamber was achieved by using turbo-molecular pumping system. Undoped and Al-, Ga- and In-doped ZnO films were deposited under oxygen partial pressure ranging from 1×10^{-3} to 5×10^{-4} Torr. The deposition temperatures were between 450 and 520 °C and deposition time is from 50 to 90 minutes. Al and In of 4N purity and Ga of 5N purity were used for doping. The Al and In targets were placed on the target holder and ablated for 15 seconds at every five-minute interval. The liquid Ga metal was placed in a glass container in the deposition chamber. The Al, Ga, and In doping concentration in the ZnO films determined from the energy-dispersive x-ray analysis is 3.53, 1.33, and 1.07 at. %, respectively. The growth conditions are given in Table 1 for these ZnO samples. The ZnO samples were post-annealed at 600 °C for 3 hrs under oxygen atmosphere at a flow rate of 18 bars. The values of the surface roughness determined by the AFM images of the ZnO samples before and after annealing are presented in the last two columns in Table 1. These values are influenced by the deposition and annealing conditions, and also correlate with the resistivity value of the films as discussed in the following. It is observed that the Al-doped and undoped ZnO film shows the highest and lowest, respectively, surface roughness after annealing. The high surface roughness of the Al- and In-doped ZnO samples after annealing may be due to that some Al and In atoms remain in the interstitial region in the annealed ZnO films.

Table 1. Deposition conditions and surface roughness values of PLD-grown undoped and Al-, Ga- and In-doped ZnO films.

ZnO sample	O_2 pressure (10^{-3} Torr)	substrate temp. (°C)	deposition time (min.)	surface roughness (nm) before annealing	surface roughness (nm) after annealing
undoped	0.5	513	50	240	6
Al-doped	2.0	500	90	220	71
Ga-doped	5.0	520	90	67	9
In-doped	2.0	450	60	201	47

The structure and the crystalline quality of the ZnO films were studied by XRD with Cu K_α source (λ=1.5406 Å). The microstructure, surface roughness, and topology of the ZnO films were obtained from the AFM images. The polarizer and analyzer angles of our single-wavelength

(λ=590 nm) ellipsometer were measured, and the values of the amplitude Ψ and the phase Δ were calculated. These two values were fed into a program based on a three-layer (air, film, and substrate) model [19]. Values of the refractive index (n), extinction coefficient (k), and thickness (d) were obtained. The optical transmittance spectra for ZnO films were recorded using a UV-Visible spectrophotometer in the range of 200-850 nm for quartz substrate and 340-850 nm for glass substrate. Since glass absorbs below 340 nm and the light source changes at 860 nm, these wavelength regions were carefully avoided in analyzing the spectra. The n value was calculated from a modified envelope method based on the simulation of the maxima and minima of the optical transmittance spectra in the region above the absorption edge under the assumption that the ZnO films do not absorb in this region [20]. Electrical resistivity and Hall mobility (with an applied magnetic field of 3 kOe) of the ZnO films were measured at 300 K by the Van der Pauw technique. The Au/Al Ohmic contacts were applied at the four corners of the square-shaped ZnO samples. Photoconductivity measurements were performed at 10 K on bar-shaped samples with Au/Al Ohmic contact at the two ends. The ZnO samples were mounted on the cold head of an APD Cryogenics Displex closed-cycle helium cryostat and were illuminated by light with photon energy of 0.6 to 1.4 eV through an Oriel 0.25-meter monochromator. Suitable band-pass filters were used to cut second-order diffracted light from the monochromator.

3. Results and discussions

Fig. 1 shows the normalized XRD spectra for undoped and Al-, Ga- and In-doped as-deposited ZnO films grown by PLD. The XRD patterns indicate good crystalline quality, and the hexagonal (002) is the only diffraction peak for all the ZnO films. No signal of the dopant metals or their oxides can be detected, which is attributed to the good crystal formation of the ZnO films during deposition [21]. Thus, doping of Al, Ga, or In does not change the orientation of the ZnO films. The stability of the hexagonal orientation of ZnO single crystal up to 12.5% Ga doping was reported by Ren et. al. [22]. Decrease in the (002) peak intensity is observed for the doped samples. In-doped ZnO film shows a large decrease of the (002) peak intensity, which may be due to the lower growth temperature (450 °C). It is also observed in Fig. 1 that doping does affect both the (002) peak position and peak width. The (002) peak shifts 0.04 and 0.06°, respectively, towards higher angles in the Al- and Ga-doped ZnO samples with respect to that of the undoped film. This is due to the slight decrease of bond length by doping with smaller-sized Al or Ga atoms. The shift of the (002) peak 0.08° towards lower angle for the In-doped ZnO film compared with the undoped one indicates the increase in the inter-atomic spacing when bigger-sized In atoms are added in the ZnO film. We note that the atomic radius for Al, Zn, Ga, and In is 1.26, 1.31, 1.26, and 1.44 Å, respectively. It is also clear from Fig. 1 that the (002) peak broadening is most pronounced in the In-doped than the Al- and Ga-doped ZnO films. This is due to the poorer crystallinity of the In-doped ZnO film associated with the lower growth temperature.

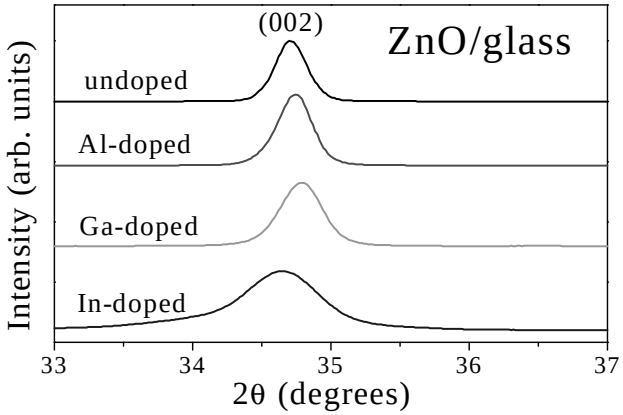

Fig. 1. XRD pattern of undoped and Al-, Ga- and In-doped as-deposited ZnO films.

The optical transmittance spectra for undoped and Al-, Ga- and In-doped as-deposited ZnO films are shown in Fig. 2. The low transmittance for the undoped and Al- and Ga-doped ZnO films may be due to the fact that excess Zn ions exist in the interstitial sites and they absorb light. These excess Zn ions also create defect levels as observed in the photoconductivity experiment discussed below. Besides, the transmittance of the ZnO films increases with Ga or In doping while decreases with Al doping in the visible range. This effect is attributed to more Al ions exist in the ZnO sample than Ga or In ions do in the respective sample, which is also confirmed by the EDX analysis. These excess Al ions absorb or reflect more visible light in the Al-doped ZnO film. The absorption edges for the Ga- and In-doped ZnO films shift towards lower wavelengths compared with that of the undoped sample. This observed blue shift indicates an increase in the band gap (E_g) and is attributed to the Burstein-Moss effect [23,24]. Doping group III metals in an n-type material causes a shift in the Fermi level, and thus E_g value increases. However, Al doping in ZnO films seems to be less effective in causing such a blue shift and, instead, a slight red shift is observed. This change in the absorption edge is important in window layer coating since it can help prevent unwanted absorption in the luminous spectra range. The E_g values of the ZnO films are determined from the peak wavelength values of the differential transmittance vs. wavelength curves, which are shown in Fig. 3. The E_g values thus calculated for undoped and Al-, Ga- and In-doped ZnO film are 3.24, 3.10, 3.40, and 3.25 eV, respectively. They are listed in the last column in Table 2. These values agree with those obtained from the usual $(\alpha h\nu)^2$ vs. $h\nu$ curves. E_g value of 3.3 eV was reported for the sputter-grown Ga-doped ZnO film [23]. The variation of n value with wavelength in the region 500-800 nm for undoped and doped ZnO films is shown in Fig. 4. The decrease of the n values in the visible region for the doped ZnO films compared with the undoped one correlates with the corresponding increase in transmittance. Similar trend was reported for sputtered ZnO films [24]. Dispersion of n values for the ZnO films decreases exponentially, which is typical for a semiconductor. The Al-doped ZnO film shows the largest n value. It is noted that the n values obtained from the ellipsometry experiment are smaller than those measured by spectrophotometry for the Al- and Ga-doped ZnO films. This is due to the assumption made in the latter experiment that the absorption is zero. Furthermore, the spectrophotometry evaluation of the n values does not include the phase variation. The n values determined by ellipsometry and spectrophotometry at a specific wavelength of 590 nm are given in Table 2. In Table 2, the thickness of the ZnO films is about 1 μm and the k values are very small, which indicates that the absorption of the ZnO films at λ=590 nm is negligible. This finding justifies our assumption made earlier in the calculation of n values from the spectrophotometry data that ZnO films do not absorb in the visible range.

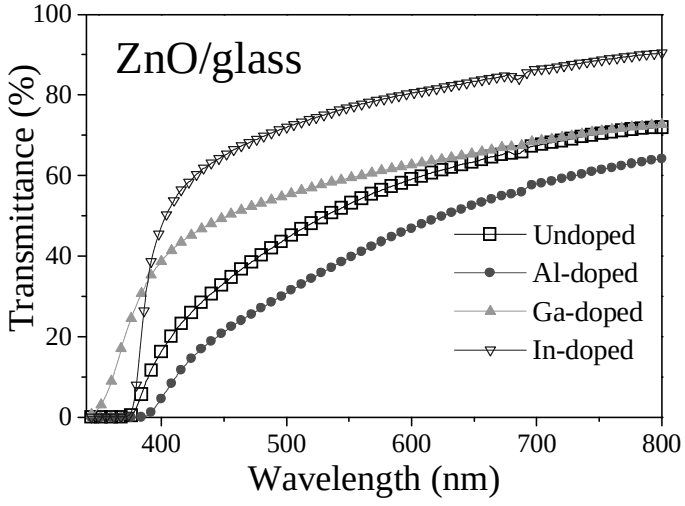

Fig. 2. The optical transmittance spectra for undoped and Al-, Ga- and In-doped as-deposited ZnO films.

Table 2. Values of d, n, and k calculated by ellipsometry and the n and E_g values determined from spectrophotometry of undoped and doped ZnO films.

ZnO sample	ellipsometry			spectrophotometry	
	d (nm)	n	k	n	E_g
undoped	910	2.15	0.090	2.30	3.24
Al-doped	970	2.01	0.064	2.71	3.10
Ga-doped	910	2.02	0.060	2.18	3.40
In-doped	1070	1.96	0.065	1.72	3.25

In Fig. 2, the transmittance increases with wavelength in the visible region. However, the ZnO films begin to reflect in the near IR region and the transmittance starts to decrease at a particular wavelength λ_{min} (not shown in Fig. 2) [25]. The λ_{min} value is used to determine the plasma frequency ω_p by

$$\omega_p = \frac{2\pi c}{\lambda_{\min}} \sqrt{\frac{\varepsilon_\alpha - 1}{\varepsilon_\alpha}}, \tag{1}$$

where c is the velocity of light, and ε_α is the high-frequency dielectric constant. The λ_{min} value for the undoped, Al-, Ga-, and In-doped ZnO thin films is 810, 1002, 745, and 1143 nm, respectively. Using reported value of ε_α=4, [9] one obtains the plasma frequency ω_p for the undoped, Al-, Ga-, and In-doped ZnO thin films as 2.0×10^{15}, 1.6×10^{15}, 2.2×10^{15}, and 1.4×10^{15} s^{-1}, respectively. The electron concentration N_e is related to ω_p by

$$\omega_p^2 = \frac{N_e e^2}{\varepsilon_0 m^* (\varepsilon_\alpha - 1)} - \gamma^2, \tag{2}$$

where e is the electronic charge, ε_0 is the permitivity of free space, γ is the Drude scattering frequency at which the free carriers are scattered, and m^*=0.23 m_0 (m_0 is the electron static mass) [26]. The estimated γ value for ZnO is 1.5×10^{14} sec^{-1} [25]. The N_e values for the ZnO films thus calculated are presented in the last column in Table III. It is observed that the Drude scattering contribution is very small in all our ZnO films. The N_e value for the Al-doped ZnO film (5.6×10^{20} cm^{-3}) is about half of that (1.2×10^{21} cm^{-3}) [9] reported previously. The Ga-doped ZnO sample has the highest electron concentration of about 1×10^{21} cm^{-3}, which is comparable to that (3.77×10^{20} cm^{-3}) [27] reported earlier. Furthermore, the relationship of electron concentration and the Fermi level can be written as

$$N_e = 2(2\pi m^* kT/h^2)^{3/2} \exp[(E_F - E_C)/kT], \tag{3}$$

where N_e is the electron concentration, m^* is the electron effective mass in the conduction band, k is the Boltzmann constant, T is the absolute temperature, h is the Planck's constant, E_F and E_C are the energies at the Fermi level and bottom of conduction band, respectively. Using the N_e values in Table 3 and m^*=0.23 m_0, [26] one obtains that the Fermi level of undoped, Al-, Ga- and In-doped ZnO film is 149, 138, 154, and 131 meV, respectively, below the respective conduction band. These values are comparable to that (120 meV) reported for the Ga-doped ZnO film [27].

Table 3. Electrical resistivity, Hall mobility, and electron concentration of ZnO thin films measured at 300 K.

ZnO sample	resistivity (10^{-4} Ω-cm)	mobility (cm^2/Vs)	N_e (10^{20} cm^{-3})
Undoped			8.7
Al-doped	27.3	4	5.6
Ga-doped	2.9	20	10.5
In-doped	26.8	5	4.3

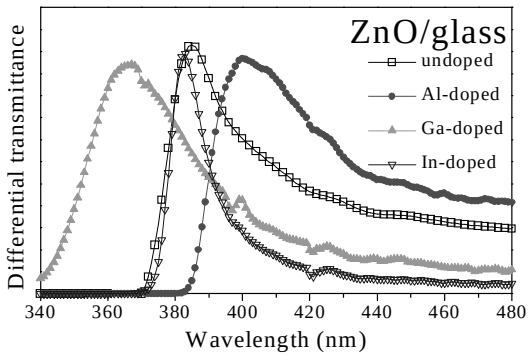

Fig. 3. Differential transmittance spectra for the samples of Fig. 2.

The electrical resistivity and Hall mobility values of the doped ZnO films measured at 300 K are listed in Table 3. No reliable Hall measurement could be performed for the undoped ZnO film due to the very high resistance, which may be due to large deficiency of oxygen vacancies. We note that the electron concentrations obtained from the Hall measurement of ZnO films are essentially the same as those obtained from the above optical measurement. The Ga-doped ZnO film has the lowest resistivity (2.9×10^{-4} Ω-cm) and highest mobility (20 cm^2/Vs) value, which is comparable to the corresponding value (8.9×10^{-4} Ω-cm and 18.5 cm^2/Vs) [27] reported previously. It is clear that doping ZnO thin film with Al, Ga, or In significantly reduces the resistivity with much higher mobility. The higher resistivity and lower mobility values for Al- and In-doped ZnO films is due to the degradation of crystallinity with decrease of oxygen partial pressure (see Table 1). The electrical resistivity of the ZnO films is also roughness dependent. The less rough is the surface, the less resistive is the film. As shown in Tables 1 and 3, the Ga-doped ZnO film shows the lowest resistivity and surface roughness values among these ZnO samples. The surface roughness and resistivity measurements on RF-sputtered ZnO thin films also confirm this assertion [24].

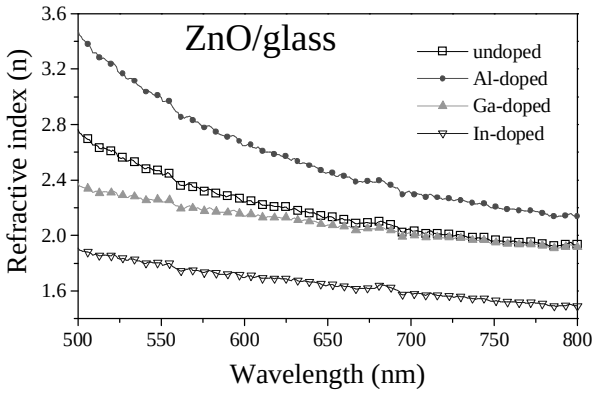

Fig. 4. Wavelength dependence of the refractive indices of undoped and Al-, Ga- and In-doped as-deposited ZnO films.

Photoconductivity spectra measured at 10 K for the undoped and doped ZnO samples are shown in Fig. 5. The spectrum of the undoped ZnO film is characterized by a broad structure in the photon energy range of 0.8 to 1.1 eV. This broad peak is due to the emission of charge carriers from various deep-level traps present in this sample. For the doped ZnO films, one identifies rather distinct photoconductivity peaks and shoulders corresponding to deep levels with various energies between 0.75 and 1.14 eV. The Al-, Ga-, and In-doped ZnO film possesses deep levels corresponding to (0.89, 1.01, and 1.14), (0.75 and 1.01), and (0.83, 0.89, 1.01 and 1.14) eV, respectively. Besides the 0.75 eV trap, all the other traps seem to appear in the undoped ZnO film under the broad structure in varying proportions. We note that ZnO is known to contain several electron and hole traps with energies ranging from 0.05 to 0.9 eV [28,29]. The origin of some of the traps remained unclear although it was recognized that the dual charge states of Zn interstitials and oxygen vacancy are responsible for some of the defect levels in ZnO [29]. The 0.83 and 0.89 eV traps are most pronounced in the In-doped, very less in the Al-doped, and almost non-existent in the Ga-doped ZnO film. It was stated earlier [30] that the difference in bond lengths of In-O and Zn-O is substantially higher than that of Ga-O and Zn-O. This results in a much higher strain and crystal deformation in the In-doped than that in the Ga-doped ZnO film. This fact is used to assign the 0.83 and 0.89 eV traps to crystal deformations in ZnO. We note that a hole trap with activation energy of 0.78 eV was found in proton-irradiated ZnO and its origin was related to crystal defects [31]. Our observed 0.83 eV trap may be this hole trap. Similarly, a hole trap with activation energy of 0.9 eV was observed earlier in bulk ZnO and was related to point defects [30]. We thus assign our observed 0.9 eV trap with this trap. Furthermore, Studenikin et. al., [32] detected hole traps with energies near 1 eV from photoconductivity transient measurement. This 1 eV trap appears to have highest concentration in our Ga-doped ZnO film, and lower concentration in our Al- or In-doped ZnO films. Considering the growth temperatures of 500, 520, and 450 °C, respectively, for the Al-, Ga-, and In-doped ZnO films in Table 1, we assign this 1-eV trap to native defects in our ZnO films, which are generated at high growth temperature. Finally, the 1.14 eV trap is present in all ZnO samples and is most prominent in the Al-doped ZnO film. We also performed photoconductivity measurements on undoped ZnO films deposited on glass substrate by RF sputtering at 550 °C. Two prominent peaks with energies of 1.2 and 1.35 eV were observed. The 1.2 eV peak is likely to be the same as the 1.14 eV peak in the PLD-deposited ZnO film, and might have the common origin as native defect in the ZnO films. The absence of traps with energies 0.75, 0.83, 0.89 and 1.01 eV in the sputtered ZnO films indicates that they are only related to the PLD deposition conditions.

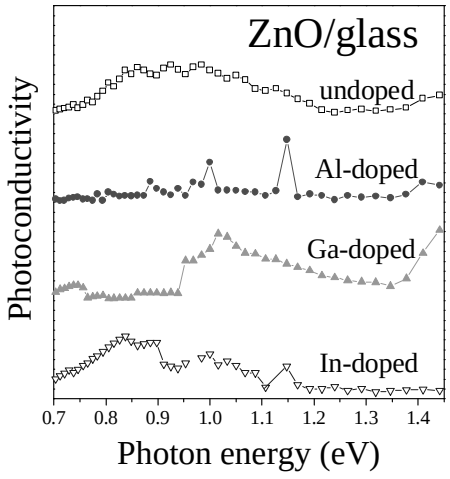

Fig. 5. Photoconductivity spectra of undoped and Al-, Ga- and In-doped as-deposited ZnO films.

4. Conclusions

Growth of undoped and Al-, Ga- and In-doped ZnO thin films on glass substrate using PLD is reported. The structure of the films remained unaffected by doping. After annealing, the surface

roughness of the ZnO films decreases. The E_g value of the undoped ZnO film is 3.24 eV, and the value increases when doped with Ga or In. Lower resistivity and higher mobility is obtained by doping the ZnO film. Photoconductivity study revealed the presence of a number of deep-level traps in the ZnO films and their possible origins were discussed.

Acknowledgements

We thank V. N. Mani for the assistance in growing the samples and D. Mardare for loaning us the ellipsometry program. This work is partially sponsored by the National Science Council, Taiwan, Republic of China.

References

[1] Z. K. Tang, G. K. L. Wong, P. Yu, M. Kawasaki, O. Ohtomo, H. Koinuma, Y. Segawa, Appl. Phys. Lett. **72**, 3279 (1998).
[2] V. Cracium, J. Elders, J. G. E Gardeniers, I. W. Boyd, Appl. Phys. Lett. **65**, 2963 (1994).
[3] S. S. Kim, B.-T. Lee, Thin Solid Films **446**, 307 (2004).
[4] L.-S. Hsu, D. Luca, J. Optoelectron. Adv. Mater. **5,** 841 (2003).
[5] M. Sumiya, A. Tsukazaki, S. Fuke, A. Ohtomo, H. Koinuma, M. Kawasaki, Appl. Surf. Sci. **223**, 2061 (2004).
[6] J. A. Sans, A. Segura, M. Mollar, B. Mari, Thin Solid Films **453**, 251 (2004).
[7] P. Bhattacharya, R. R. Das, R. S. Katiyar, Thin Solid Films **447**, 564 (2004).
[8] F. K. Shan, B. C. Shin, S. C. Kim, Y. S. Yu, J. European Ceramic Soc. **24**, 1861 (2004).
[9] A. V. Singh, M. Kumar, R. M. Mehra, A. Wakahara, A. Yoshida, J. Indian Inst. Sci. **81,** 527 (2001).
[10] T. Minami, K. Oohasi, S. Takata, T. Mouri, N. Ogawa, Thin Solid Films **193/194,** 721 (1990).
[11] T. Yamamoto, H. K. Yoshida, Jpn. J. Appl. Phys. **38**, L166 (1999).
[12] T. Yamamoto, H. K. Yoshida, Physica **B 302-303,** 155 (2000).
[13] E. S. Shim, H. S. Kang, S. S. Pang, J. S. Kang, I. Yun, S. Y. Lee, E. S. Shim, Mat. Sci. & Eng. **B102**, 366 (2003).
[14] A. Zeuner, H. Alves, D. M. Hofmann, B. K. Meyer, A. Hoffmann, G. Kaczmarczyk, M. Heuken, A. Frost, J. Blasing, phys. stat. solidi (b) **229**, 907 (2003).
[15] T. Ohshima, T. Ikegami, K. Ebihara, J. Asmussen, R. K. Thareja, Thin Solid Films **435,** 49 (2003).
[16] F. K. Shan, Y. S. Yu, Thin Solid Films **435**, 174 (2003).
[17] T. Ohshima, R. K. Thareja, T. Ikegami, K. Ebihara, Surf. & Coat. Tech. **169**, 517 (2003).
[18] E. de Posada, G. Tobin, E. McGlynn, J. G. Lunney, Appl. Surf. Sci. **208,** 589 (2003).
[19] D. Mardare, A. Stancu, Mater. Res. Bull. **35**, 2017 (2000).
[20] R. Swanepoel, J. Opt. Soc. Am. A **2,** 1399 (1985).
[21] S. H. Jeong, J. W. Lee, S. B. Lee, J. H. Boo, Thin Solid Films **435**, 78 (2003).
[22] C. Y. Ren, S. H. Chiou, C. S. Hsue, Physica B **349,** 136 (2004).
[23] Z. F. Liu, F. K. Shan, Y. X. Li, B. C. Shin, Y. S. Yu, J. Cryst. Growth **259,** 130 (2003).
[24] X. H. Li, A. P. Huang, M. K. Zhu, S. L. Xu, J. Chen, H. Wang, B. Wang, H. Yan, Mater. Lett. **57**, 4655 (2003).
[25] T. Minami, H. Sato, H. Nanto, S. Takata, Jpn. J. Appl. Phys. **24,** L 605 (1985).
[26] M. Oshikiri, Y. Imanaka, F. Aryasetiawan, G. Kido, Physica B **298**, 472 (2001).
[27] C. X. Xu, X. W. Sun, B. J. Chen, Appl. Phys. Lett. **84**, 1540 (2004).
[28] F. D. Auret, S. A. Goodman, M. Hayes, M. J. Legodi, H. A. van Larhoven, Appl. Phys. Lett. **79**, 3074 (2001).
[29] A. Y. Polyakov, N. B. Smirnov, A. V. Govorkov, K. Ip, M. E. Overbarg, Y. W. Heo, D. P. Norton, S. J. Pearton, B. Luo, F. Ren, J. M. Zavada, J. Appl. Phys. **94**, 400 (2003).
[30] H. J. Ko, Y. F. Chen, S. K. Hong, H. Wenisch, T. Yao, D. C. Look, Appl. Phys. Lett. **77**, 3761 (2000).
[31] F. A. Kroger, The Chemistry of Imperfect Crystals (Wiley-Interscience, New York, 1964).
[32] S. A. Studenikin, N. Golego, M. Cocivera, J. Appl. Phys. **84**, 5001 (1998).